

See discussions, stats, and author profiles for this publication at: <https://www.researchgate.net/publication/51572646>

Bioaccumulation and Effects of CdTe/CdS Quantum Dots on *Chlamydomonas reinhardtii* – Nanoparticles or the Free Ions?

ARTICLE *in* ENVIRONMENTAL SCIENCE & TECHNOLOGY · AUGUST 2011

Impact Factor: 5.33 · DOI: 10.1021/es201193s · Source: PubMed

CITATIONS

45

READS

85

4 AUTHORS, INCLUDING:



Rute Domingos

Institut de Physique du Globe de Paris

28 PUBLICATIONS 765 CITATIONS

SEE PROFILE



Charles Hauser

St. Edward's University

25 PUBLICATIONS 1,702 CITATIONS

SEE PROFILE



Kevin J Wilkinson

Université de Montréal

162 PUBLICATIONS 5,073 CITATIONS

SEE PROFILE

Bioaccumulation and Effects of CdTe/CdS Quantum Dots on *Chlamydomonas reinhardtii* – Nanoparticles or the Free Ions?

Rute F. Domingos,^{*,†,‡} Dana F. Simon,[†] Charles Hauser,[§] and Kevin J. Wilkinson[†]

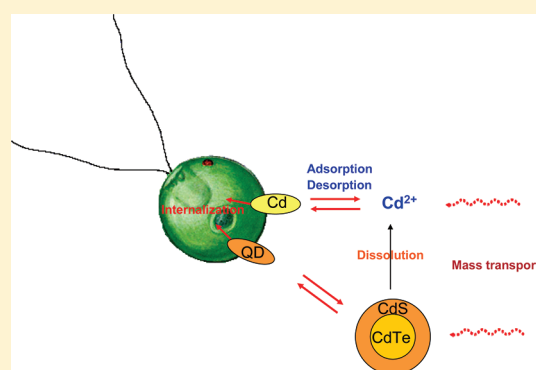
[†]Département de Chimie, Université de Montréal, C.P. 6128, succursale Centre-ville, Montréal, Quebec H3C 3J7, Canada

[‡]Centro de Química Estrutural, Instituto Superior Técnico/Universidade Técnica de Lisboa, Torre Sul lab 11-6.3, Av. Rovisco Pais # 1, 1049-001 Lisbon, Portugal

[§]Bioinformatics Program, St. Edward's University, Austin, Texas 78704, United States

 Supporting Information

ABSTRACT: In order to properly assess the environmental risk of engineered nanoparticles (ENP), it is necessary to determine their fate (including dissolution, aggregation, and bioaccumulation) under representative environmental conditions. CdTe/CdS quantum dots (QD), such as those used in medical imaging, are known to release Cd²⁺ due (mainly) to the dissolution of their outer shell. In this study, *Chlamydomonas reinhardtii* was exposed to either a soluble Cd salt or QD at similar concentrations of total Cd. Free Cd concentrations were measured using the *Absence of Gradients and Nernstian Equilibrium Stripping* technique. QD dissolution increased with decreasing pH and with increasing QD concentration. When exposed to QD, bioaccumulation was largely accounted for by dissolved Cd. Nonetheless, QD were shown to be taken up by the cells and to provoke unique biological effects. Whole transcriptome screening using RNA-Seq analysis showed that the free Cd and the QD had distinctly different biological effects.



INTRODUCTION

Nanotechnology has shown great promise in the fields of medicine, energy production, and environmental remediation, due to the unique properties that many materials possess when manufactured at the nanometer scale. Quantum dots (QD) are of great interest due to their tunable optical properties.^{1,2} Their high photostability makes these nanomaterials advantageous over conventional fluorophores for long-term biological and multi-target imaging. Although the current market for QD is small, it is growing rapidly as novel applications are developed.³ Like other classes of engineered nanoparticles (ENP), QD may ultimately find their way into the environment.

A typical QD is composed of a semiconductor core (e.g., CdSe, CdTe) that can be encapsulated in a shell (e.g., CdS) to enhance both optical and electronic properties while reducing core metal leaching.⁴ Some QD have organic coatings that increase their dispersion in water and help direct them to biological targets.⁵ Many of the particles have been found to degrade under photolytic or oxidative conditions.^{4,6,7} Given the high potential for toxicity of the released Cd,⁸ it is necessary to precisely quantify both particle dissolution and whether or not the intact QD have their own effects, independent of the Cd²⁺. Indeed, several reports have demonstrated a toxicity of either the composite core^{9–13} or the QD surface coating.^{14–16} Furthermore, some studies have shown that particle sizes^{16–18} may influence the toxicity of the QD, with smaller sizes generally being more cytotoxic. Clearly, understanding the physicochemical properties

of the QD, including their aggregation and dissolution, is fundamental to evaluate their environmental risk. Key to that evaluation is a determination of whether intact NPs are able to cross biological membranes and/or induce independent biological effects. While several mechanisms are known to allow NPs to enter plant cells (binding to carrier proteins, aquaporins, ion channels, endocytosis, or the creation of new pores),¹⁹ it is not known why the uptake of NPs appears to be selective to only certain organisms.

The objective of this work was thus to evaluate the uptake and effects of a carboxylate terminated CdTe/CdS QD in comparison to Cd²⁺ for a unicellular green alga, *Chlamydomonas reinhardtii*. Special emphasis was placed on i) precisely quantifying Cd²⁺ concentrations; ii) determining the role of pH on the dissolution of the QD; iii) determining whether the QD were accumulated by the alga, and, if so, iv) whether particle size influenced bioaccumulation. Finally, transcriptomic profiling (v) was used to determine whether the effects of the QD were due simply to the exposure of the algae to dissolved Cd²⁺.²⁰

EXPERIMENTAL SECTION

Algal Growth and Experimental Media. The unicellular green alga, *C. reinhardtii* (wild type C137) employed in this study,

Received: April 8, 2011

Accepted: August 15, 2011

Revised: August 1, 2011

Published: August 15, 2011

is a model organism amenable to genetic, biochemical, and reverse genetic manipulation whose genome has been completely sequenced.²¹ *C. reinhardtii* was transferred from a week-old tris-acetate-phosphate (TAP) agar plate²² into a (4×) diluted TAP media ($I = 10^{-2}$ M).²³ Cells were grown in an incubation chamber (Infors) at 22 °C, under a 12:12 h light:dark regime under fluorescent lighting ($80 \mu\text{mol}$ of photons $\text{m}^{-2} \text{s}^{-1}$) and rotary shaking (100 rpm) to a density of $(2-3) \times 10^6$ cells mL^{-1} (generally after 4 days). Cells were diluted to 10^5 cells mL^{-1} in fresh media, grown to midexponential growth ($(1-3) \times 10^6$ cells mL^{-1} , more 4 days), and harvested by centrifugation ($3700 \times g$, 4 min) in 50 mL of sterile (polypropylene) centrifuge tubes. The cell pellet was washed ($2\times$) and centrifuged with free-metal experimental medium (see below). Cell densities, sizes, and surface distributions were determined using a Coulter Multisizer 3 particle counter (50 μm orifice, Coulter Electronics).

The experimental media contained 2×10^{-2} M MES (2-(N-morpholino)ethanesulfonic acid, Sigma) for experiments performed at pH 6 and 6.5, 2×10^{-2} M HEPES (4-(2-hydroxyethyl)-piperazine-1-ethanesulfonic acid, Sigma) for experiments run at pH 7.0 and 7.5 and 2×10^{-2} M MOPS (3-(N-morpholino)-propanesulfonic acid, Sigma) when experiments were performed at pH 8.0. Ca ($\text{Ca}(\text{NO}_3)_2 \cdot 4\text{H}_2\text{O}$, 10^{-5} M, Sigma) was added to each buffer solution in order to maintain cell wall integrity.²⁴ The pH was adjusted using HNO_3 (trace select ultra grade, Fluka) or NaOH (analytical grade, ACP). Culture media and experimental solutions were sterilized (autoclaved and filtered over 0.2 μm filters where appropriate); bottle borders were flame sterilized, and algal cultures were manipulated under laminar flow. Polycarbonate vessels were acid washed to reduce metal contamination.

Experimental solutions for the Cd bioaccumulation experiments contained between 5×10^{-9} and 5×10^{-6} M of total Cd (TraceCert grade, Fluka) in buffered media. In the absence of added ligand, Cd^{2+} accounted for >96% of total Cd. Free metal concentrations were determined from measured concentrations of dissolved Cd using thermodynamic calculations (Visual MINTEQ version 2.5.3²⁵).

Bioaccumulation experiments using the QD were performed for total Cd concentrations ranging between 2×10^{-7} and 4×10^{-6} M. Three different sizes (and corresponding colors) of CdTe/CdS carboxyl-terminated QD (Vive Nano Inc.) were employed: orange (QDO), yellow (QDY), and green (QDG). Accordingly with the manufacturer, the three QD are prepared from the same CdTe core (diameter of 3–4 nm). QDO and QDY are made by adding slightly increased CdS shell to the QDG. The largest (orange) QD was studied at all pH, whereas the QDG and the QDY were only studied at pH 7.0. Controls experiments were performed using solutions that were prepared in exactly the same manner as the solutions containing Cd or QD.

All exposure solutions were equilibrated 24 h prior to use. Bioaccumulation was examined in short-term experiments (0, 15, and 30 min) in order to decrease the likelihood of modification to the experimental media due to complexation by algal exudates or metal depletion.²⁴ Metal biouptake was stopped by adding 5 mL of 10^{-2} M EDTA (ethylenediamine-tetraacetic acid, Sigma grade) that was prepared in an identical pH buffer as the experimental medium.²⁶ **Cellular Cd** concentrations were determined on 50 mL of filtered (3.0 μm nitrocellulose, Millipore), washed (10^{-2} M EDTA in pH buffer) algae that were digested until solutions became colorless (0.3 mL of ultrapure HNO_3 at 85 °C). **Dissolved Cd** concentrations were determined from a small aliquot of filtrate sampled prior to the addition of EDTA.

Total, dissolved, and cellular Cd concentrations were quantified by graphite furnace atomic absorption spectrometry (Thermo M Series GF95Z). Total and cellular Te concentrations were quantified by ICP-MS (XserieII, Thermo).

Cd mass balances were performed by taking into account total, dissolved, and cellular metal concentrations. Data were rejected when mass balances were outside $100 \pm 5\%$. In order to evaluate biological and analytical variability, biouptake experiments consisted of a duplicated format that was repeated on three different days with freshly prepared samples and algal cultures, i.e. 3×2 samples per data point. All data are presented as a function of measured (rather than nominal) metal concentrations, unless explicitly stated.

QD Dissolution. Cd^{2+} concentrations were determined using the *Absence of Gradients and Nernstian Equilibrium Stripping* (AGNES) technique.²⁷ More detailed theory and experimental details on the AGNES technique has been provided in the Supporting Information (SI). Experiments were performed with an Eco Chemie $\mu\text{Autolab III}$ potentiostat using a Metrohm 663VA stand and GPES 4.9 software (Eco Chemie). The electrometer input impedance of this instrument is larger than 100 G Ω . A static mercury drop electrode (Merck mercury p.a., drop radius 1.41×10^{-4} m) was used as the working electrode in concert with a saturated calomel reference electrode with a 0.1 M NaNO_3 salt bridge and a glassy carbon counter electrode. AGNES experiments were calibrated using 2×10^{-6} M Cd at low pH (<4), in order to avoid losses to the container walls. Experiments were performed in triplicate using identical sample volumes (20 mL). Due to the extended length of time required to perform a given measurement, quantification was performed on experimental solutions that had been prepared in an identical manner to those used in the biouptake experiments.

Characterization of the QD. The adsorption and drop deposition methods were used to prepare QD samples for atomic force microscopy (AFM).^{28,29} For the adsorption method, freshly cleaved muscovite mica sheets were suspended in exposure solutions containing the QD for 20 min. Following their removal, the mica sheets were gently rinsed by immersion in deionized water. For the drop deposition technique, 5 μL of sample was pipetted onto freshly cleaved mica and then allowed to dry overnight in an enclosed Petri dish. Observations were performed on an AFM Digital Instruments Nanoscope IIIa extended (Dimension 3100).

Whole Transcriptome Profiling. Transcriptomic profiles for *C. reinhardtii* were generated using the SOLiD system (Applied Biosystems). Three experimental conditions were examined: i) control (no Cd or QD); ii) 5×10^{-7} M of dissolved Cd; or iii) 10^{-6} M QDG, all at pH 7 in 2×10^{-2} M HEPES buffer supplied with 10^{-5} M of $\text{Ca}(\text{NO}_3)_2 \cdot 4\text{H}_2\text{O}$. After the addition of 10^{-2} M EDTA²⁶ to stop the biouptake, cells were separated by centrifugation ($3700 \times g$, 4 min at 4 °C). Cell pellets were stored at -80 °C until required. RNA extraction and purification was accomplished by first vortexing the cells in the presence of glass beads and then purifying the RNA with a Qiagen RNeasy kit (Qiagen, Valencia, CA, USA). RNA quality and quantity were estimated from absorbance measurements at 280 and 260 nm and by analysis of the intactness of rRNA using an Agilent 2100 BioAnalyzer (Agilent Technologies, Foster City, CA, USA). RNA quality was considered acceptable when the 28S rRNA/18S rRNA ratio was ≥ 2 . Poly-(A)⁺ RNA was isolated from total RNA using the polyAtract mRNA kit (Z5300, Promega), and it was also analyzed with the Bioanalyzer. SOLiD analysis³⁰ was

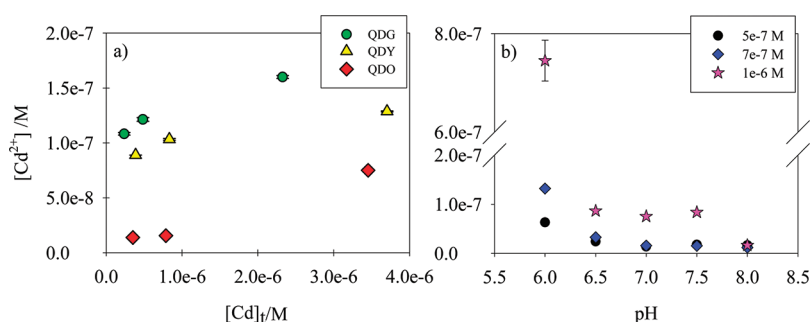


Figure 1. Cd^{2+} concentrations determined by AGNES for QD exposure solutions containing different (measured) total Cd concentrations: (a) QDO (red), QDG (green), and QDY (yellow) at pH 7.0. (b) QDO at various pH values for different nominal Cd concentrations 5×10^{-7} (black), 7×10^{-7} (blue), and 1×10^{-6} M (pink); actual measured total concentrations are provided in Table S1 in the SI.

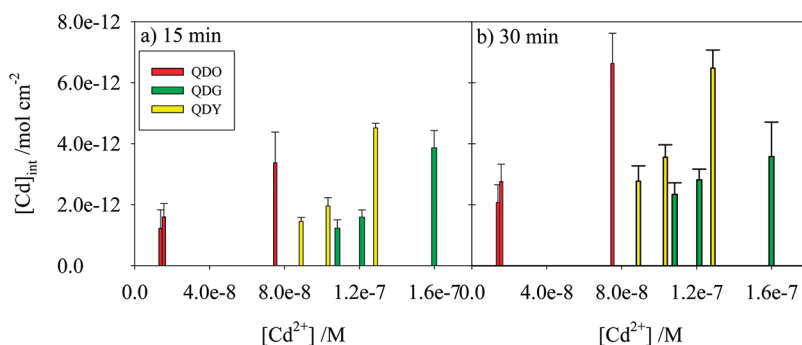


Figure 2. Cellular Cd as function of Cd^{2+} concentrations measured for QDO (red), QDG (green), and QDY (yellow) at pH 7.0. Cells were exposed to the QD for either 15 (a) or 30 (b) minutes.

performed on 150 ng of purified poly-(A)⁺ RNA. Sequences were mapped to the *C. reinhardtii* reference transcriptome using the software MAQ (<http://maq.sourceforge.net>).^{21,31} Differential gene expression was determined from the number of mapped reads that overlapped with annotated *C. reinhardtii* transcripts as the input for the DESeq package.³² Genes were considered as differentially expressed (DE) if they had a >2 fold change (either up or down regulation) and <10% false discovery rate. Enrichment of Gene Ontology (GO) categories among DE genes was determined using GSeq.³³

RESULTS AND DISCUSSION

QD Characterization. Due to the formation of a film on the mica surface, it was not possible to quantify the QD diameters in their pH buffers, and thus observations were performed in water. Number average diameters obtained from AFM height measurements gave the following: 5.7 ± 0.4 nm (QDO), 4.3 ± 0.4 nm (QDG), and 4.2 ± 1.2 nm (QDY). The value obtained for the QDO is in good agreement with previously reported values by both AFM (5.9 ± 3.4 nm) and TEM (6.5 ± 1.9 nm).³⁴

QD Dissolution. Cd^{2+} (quantified by AGNES) increased with increasing concentrations of the QD (Figure 1a) and with decreasing pH (Figure 1b). Similar concentrations of Cd^{2+} were measured for the smaller green and yellow QD, whereas the larger orange QD released less Cd. These observations are consistent with theoretical equilibrium solubility and particle dissolution rates, which are known to increase with decreasing particle size.³⁵ Additionally, for a given Cd concentration, the larger QD have proportionally more of the more easily solubilized

outer shell. Mass balance calculations indicated that the Cd^{2+} concentration corresponded to a relatively small proportion of the total Cd in solution, ranging from 0.3% (exposure solution containing the highest concentration of QDO at pH 8.0) to 21.7% (exposure solution containing the lowest concentration of QDG at pH 7.0).

Cd Biouptake. *C. reinhardtii* was exposed to QD for either 15 or 30 min and then washed with EDTA in order to remove extracellular Cd.²⁶ Cellular Cd concentrations increased with increasing QD concentrations in the medium (reflected by the $[Cd^{2+}]$; Figures 2 and 3) and with time (cf. Figure 2a and 2b; Figure 3a and 3b). Furthermore, a decrease in pH resulted in increased Cd internalization (Figure 3), consistent with the increased dissolution that was observed at the lower pH (Figure 1b). While, for a given QD, bioaccumulation varied with the concentration of dissolved Cd^{2+} ; for a given Cd^{2+} concentration, much more Cd bioaccumulation occurred from solutions containing the QDO as compared to either the QDG or the QDY (Figure 2). In other words, Cd^{2+} was a poor predictor of Cd bioaccumulation for the samples containing QD.

Bioaccumulation experiments were also performed using a soluble Cd salt in order to distinguish the uptake of free Cd ions from that of the intact QD. A linear increase of the (log) Cd internalization fluxes was observed as a function of the (log) Cd^{2+} concentrations (determined by Visual MINTEQ) (slope = 0.87 ± 0.06 , $r^2 = 0.92$ for $[Cd^{2+}] < 1 \times 10^{-6}$ M at pH 7.0; Figure 4a). On a log–log graph, a slope of unity implies that uptake is directly proportional to the free ion or surface bound metal concentrations (Equation S3 of Supporting Information), as would be predicted by either the Free Ion Activity Model or

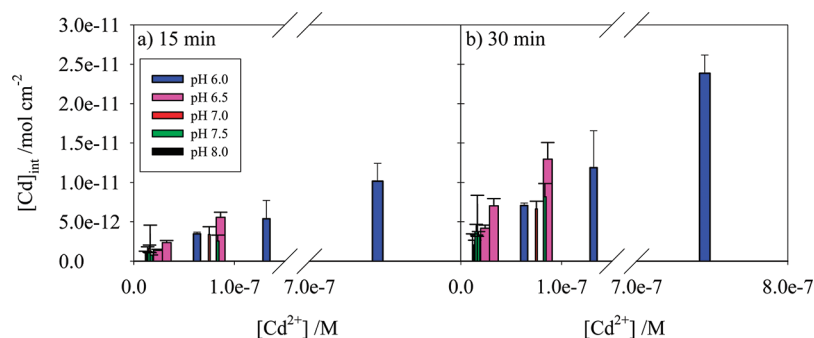


Figure 3. Cellular Cd as function of Cd^{2+} concentrations measured for QDO at pH 6.0 (blue), 6.5 (pink), 7.0 (red), 7.5 (green), and 8.0 (black). Cells were exposed to the QD for either 15 (a) or 30 (b) minutes. The lower Cd^{2+} concentrations have been expanded in Figure S1 in the SI.

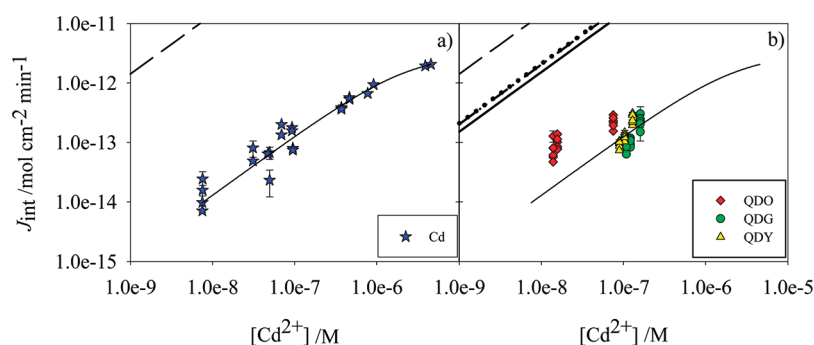


Figure 4. Internalization flux as a function of Cd^{2+} for *C. reinhardtii* at pH 7.0. (a) Cd (blue); the bold long dash line represents the calculated maximal diffusive flux for Cd. (b) QDO (red), QDG (green), and QDY (yellow); the bold lines represent the calculated maximal diffusive flux for QDO (solid), QDG (dash-dot-dot), QDY (dotted), and Cd (long dash). In both graphs the thin line represents a Michaelis–Menten plot.

the Biotic Ligand Model.³⁶ Figure 4 demonstrates clearly that Cd uptake **was not** mass transport limited. Indeed, the maximum diffusive flux of free Cd (Figure 4a: long dashed line), calculated from Fick's second law for the steady-state, radial diffusion of Cd^{2+} ($D_{\text{Cd}^{2+}} = 7.0 \times 10^{-10} \text{ m}^2 \text{ s}^{-1}$,³⁷) toward an organism with a radius of $3.5 \times 10^{-4} \text{ cm}$,³⁸ was 3 orders of magnitude larger than the observed internalization flux, implying that the diffusive supply of Cd^{2+} was more than sufficient to sustain uptake. Figure 4a demonstrates clearly that Cd uptake was limited by the rate of the Cd internalization flux, similar to previous observations,²³ and consistent with the Biotic Ligand Model.³⁶

Intuitively, the presence of particles could result in reduced uptake due to a reduction in the mass transport (diffusion) of the metal to the surface of the alga. Maximum diffusive fluxes for the QD (Figure 4b) can be calculated as above, using diffusion coefficients calculated from (AFM) particle diameters. Even in the presence of the NPs, mass transport was not limiting – maximum diffusion fluxes remained almost 2 orders of magnitude larger than the observed internalization fluxes (Figure 4b).

For the green and yellow QD, Cd uptake could be predicted solely on the basis of the concentration of free ion (Figure 4b). On the other hand, for the orange QD, uptake was significantly higher than that predicted from Cd^{2+} concentrations (Mann–Whitney Rank Sum Test; differences are greater than would be expected by chance, $p = 0.018$; Figure 4b). Given that the diffusive fluxes of the QD were not limiting, the additional Cd uptake **could not** have resulted from particle dissolution at the membrane surface prior to uptake, i.e. the cells were at equilibrium with their surroundings. In other words, Cd^{2+} concentrations

at the algal surface are equal to those measured in the bulk solution. Based upon calculations of the excess internalized Cd (measured internalized Cd - predicted Cd levels determined by the Michaelis–Menten calculations described in the SI), pH had an important effect on QD bioaccumulation -0.2% of internalized Cd was attributed to the intact QDO at pH 6.0, whereas at pH 8.0, internalization of QDO was $12\times$ greater than that of the Cd^{2+} .

Two other lines of evidence were examined in order to determine whether intact QDO were internalized by the algae. First, confocal microscopy was performed in order to detect the fluorescence of the QD inside the algal cells. In this case, due to the strong autofluorescence of *C. reinhardtii*, it was impossible to detect increases in fluorescence above background for the experimental conditions used. Experiments were also performed using a mutant strain (*pc-1 y-7 cw15 arg7-8*) that does not synthesize chlorophyll;³⁹ however, in that case, the weak fluorescence signal did not exceed that of the control, even for cells exposed to very high concentrations of QD (total cadmium concentrations of 6.8×10^{-5} and $9.5 \times 10^{-5} \text{ M}$). Second, Te was measured in the cells exposed to the QDO at pH 6.5 and 7.5 (Table 1). In that case, intracellular Te was well above background levels. Furthermore, Cd/Te ratios of 7.0 in the bulk solution were similar or larger than Cd/Te ratios measured in the algae. In contrast, if Cd bioaccumulation was primarily due to the accumulation of free ion, one would expect the intracellular ratio of Cd/Te to exceed that of the whole particles. These results strongly indicate that the **orange QD were accumulated by the algal cells, though the particles may have been dissolved upon entry into the cells**. Note finally that Lin et al.¹² have previously

Table 1. Cd and Te Internalization Following a 30 Minute Exposure to the Orange Quantum Dots at pH 6.5 and 7.5

pH	$[Cd]_t / M$	$[Cd^{2+}] / M$	$[Cd]_{int} / \text{mol cm}^{-2}$	$[Te]_t / M$	$[Te]_{int} / \text{mol cm}^{-2}$	$[Cd]_{int} / [Te]_{int}$
6.5	6.6×10^{-7}	2.4×10^{-8}	1.3×10^{-11}	9.5×10^{-8}	3.0×10^{-12}	4.3
7.5	5.8×10^{-7}	1.8×10^{-8}	8.5×10^{-12}	8.3×10^{-8}	1.2×10^{-12}	7.1

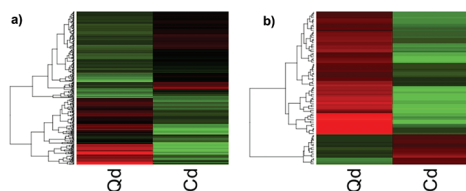


Figure 5. (a) Heat map diagram using transcripts whose expression levels are up- or down-regulated (\log_2 -fold change >1.5 with map reads of >30). (b) Heat map diagram generated with reciprocally regulated genes. The color scale in the figure depicts the fold change for each transcript, with green being indicative of upregulation, red being indicative of downregulation, and (\log_2) levels <1.5 being given in black. Expression levels were based on count reads normalized by library size for a sample ($5 \times 10^{-7} M Cd^{2+}$ or $10^{-6} M$ of QDG) compared to its control.

shown a logarithmic increase in the amount of QD that was absorbed to *Chlamydomonas sp.* as a function of the bulk concentration (0.05 – 5 mg L^{-1}) of a mercaptoundecanoic acid coated CdSe/ZnS QD. In that case, intact, internalized QD were not observed by electron microscopy following a 2 h incubation.

Transcriptomic Profiling. The above results showed that, under certain conditions, the orange QD were internalized by the algal cells to a much greater extent than could be predicted by particle dissolution. For the green and yellow QD, Cd bioaccumulation appeared to be mainly controlled by Cd^{2+} . Nonetheless, QD are thought to be surface reactive, potentially increasing oxidative stresses on the organism,⁴⁰ without necessarily crossing a biological membrane. Therefore, in order to probe whether the QD had any effects on the algae, even if they were not significantly accumulated, whole transcriptome profiling (RNA-Seq analysis by SOLiD system) was performed for the QD containing the smallest quantity of CdS shell (QDG). Transcript expression levels were compared for cells exposed to the free Cd and the QDG. Transcriptomic profiles of the cells exposed to QD were noticeably different from those exposed to Cd^{2+} . Based upon a minimum threshold of a 2.8-fold change ($\log_2 = 1.5$) in transcript expression with respect to the control (nonexposed cells), DESeq identified 174 transcripts that were specifically up-regulated by QD, 133 transcripts up-regulated by Cd^{2+} , and 86 reciprocally regulated transcripts (Figure 5).

Gene Ontology (GO) analysis identified as overrepresented, categories for oxidative-stress, redox, protein folding, and chaperone activity pathways in the Cd-treated cells (Tables S2, S3). In contrast, pathways for transmembrane activity, proteolysis involving proteasome activation, and ubiquitin-mediated processes were identified in the QD-treated cells. Screening for the 10 genes showing the greatest differential expression (DE) also revealed specific responses for Cd^{2+} and the QD (Tables S4, S5). In fact, the transcripts that were most affected by the Cd treatment did not appear to be induced by exposure to the QD (negative values for \log_2 transcript levels of the QD). In contrast, most of the genes affected by the QD treatment were also affected by the Cd treatment, albeit to a smaller extent.

The transcriptomic results contrast with a study by Gagné et al.⁴¹ that showed that, for a number of biomarker genes in rainbow trout hepatocytes, the effects of CdTe QD could be attributed to Cd^{2+} rather than the QD. Clearly, in this study, on a molecular level, the biological response and bioaccumulation observed in the presence of QD *could not simply be attributed to particle dissolution*. Somewhat counterintuitively, bioaccumulation of the particles was much greater for the largest examined QD.

Environmental Implications. The increasing release of nanomaterials has led to increased concerns about their potential environmental impacts. Dissolution was clearly important and clearly affected by the nature of the external medium (pH). Based upon this study, risk assessment of the QD will require a thorough evaluation of the quantities and effects of *both* the dissolution products and the intact QD.

■ ASSOCIATED CONTENT

Supporting Information. More information is given on the theory behind AGNES, metal transport, BLM, and the Michaelis–Menten parameters obtained for the Cd salt uptake. Tables with the measured total Cd concentrations for the QDO experiments, the Gene Ontology results, and the genes screening are also available. This material is available free of charge via the Internet at <http://pubs.acs.org>.

■ AUTHOR INFORMATION

Corresponding Author

*Phone: (+351) 21 841 9292. Fax: (+351) 21 846 4455. E-mail: rute.domingos@ist.utl.pt.

■ ACKNOWLEDGMENT

Funding for this work was provided by the *Fundação para a Ciência e Tecnologia*, Portugal (Postdoctoral fellowship to RFD (SFRH/BPD/37731/2007) and Science 2008 IST-CQE3 “Environmental Chemistry” Assistant Researcher position to RFD), the Natural Sciences and Engineering Research Council of Canada (NRC-NSERC-BDC nanotechnology initiative) and Environment Canada. The authors would like to thank Pierre Chagnon and Patrick Gendron (Genomics core facility, University of Montreal) for the RNA-Seq and Patrick Turcotte (Environment Canada) for his analysis of cellular Te.

■ REFERENCES

- Alivisatos, A. P. Semiconductor clusters, nanocrystals, and quantum dots. *Science* **1996**, *271*, 933–937.
- Alivisatos, A. P. Perspectives on the physical chemistry of semiconductor nanocrystals. *J. Phys. Chem.* **1996**, *100*, 13226–13239.
- Michalet, X.; Pinaud, F. F.; Bentolila, L. A.; Tsay, J. M.; Doose, S.; Li, J. J.; Sundaresan, G.; Wu, M.; Gambhir, S. S.; Weiss, S. Quantum dots for live cells, in vivo imaging, and diagnostics. *Science* **2005**, *307*, 538–544.
- Derfus, A. M.; Chan, W. C. W.; Bhatia, S. N. Probing the cytotoxicity of semiconductor quantum dots. *Nano Lett.* **2004**, *4*, 11–18.

- (5) Medintz, I. L.; Uyeda, H. T.; Goldman, E. R.; Mattoussi, H. Quantum dot bioconjugates for imaging, labelling and sensing. *Nat. Mater.* **2005**, *4*, 435–446.
- (6) Aldana, J.; Wang, Y. A.; Peng, X. Photochemical instability of CdSe nanocrystals coated by hydrophobic thiols. *J. Am. Chem. Soc.* **2001**, *123*, 8844–8850.
- (7) Kloepfer, J. A.; Mielke, R. E.; Wong, M. S.; Nealsen, K. H.; Stucky, G.; Nadeau, J. L. Quantum dots as strain- and metabolism-specific microbiological labels. *Appl. Environ. Microbiol.* **2003**, *69*, 4205–4213.
- (8) Mahendra, S.; Zhu, H.; Colvin, V. L.; Alvarez, P. J. Quantum dot weathering results in microbial toxicity. *Environ. Sci. Technol.* **2008**, *42*, 9424–9430.
- (9) Kloepfer, J. A.; Mielke, R. E.; Nadeau, J. L. Uptake of CdSe and CdSe/ZnS quantum dots into bacteria via purine-dependent mechanisms. *Appl. Environ. Microbiol.* **2005**, *71*, 2548–2557.
- (10) Bouldin, J. L.; Ingle, T. M.; Sengupta, A.; Alexander, R.; Hannigan, R. E.; Buchanan, R. A. Aqueous toxicity and food chain transfer of quantum dots in freshwater algae and *Ceriodaphnia dubia*. *Environ. Toxicol. Chem.* **2008**, *27*, 1958–1963.
- (11) Wang, J.; Zhang, X.; Chen, Y.; Sommerfeld, M.; Hu, Q. Toxicity assessment of manufactured nanomaterials using the unicellular green alga *Chlamydomonas reinhardtii*. *Chemosphere* **2008**, *73*, 1121–1128.
- (12) Lin, S.; Bhattacharya, P.; Rajapakse, N. C.; Brune, D. E.; Ke, P. C. Effects of quantum dots adsorption on algal photosynthesis. *J. Phys. Chem. C* **2009**, *113*, 10962–10966.
- (13) Priester, J. H.; Stoimenov, P. K.; Mielke, R. E.; Webb, S. M.; Ehrhardt, C.; Zhang, J. P.; Stucky, G. D.; Holden, P. A. Effects of soluble cadmium salts versus CdSe quantum dots on the growth of planktonic *Pseudomonas aeruginosa*. *Environ. Sci. Technol.* **2009**, *43*, 2589–2594.
- (14) Guo, G.; Liu, W.; Liang, J.; He, Z.; Xu, H.; Yang, X. Probing the cytotoxicity of CdSe quantum dots with surface modification. *Mater. Lett.* **2007**, *61*, 1641–1644.
- (15) Ryman-Rasmussen, J. P.; Riviere, J. E.; Monteiro-Riviere, N. A. Surface coatings determine cytotoxicity and irritation potential of quantum dot nanoparticles in epidermal keratinocytes. *J. Invest. Dermatol.* **2007**, *127*, 143–153.
- (16) Lovric, J.; Cho, S. J.; Winnik, F. M.; Maysinger, D. Unmodified cadmium telluride quantum dots induce reactive oxygen species formation leading to multiple organelle damage and cell death. *Chem. Biol.* **2005**, *12*, 1227–1234.
- (17) Zhang, Y. B.; Chen, W.; Zhang, J.; Liu, J.; Chen, G. P.; Pope, C. In vitro and in vivo toxicity of CdTe nanoparticles. *J. Nanosci. Nanotech.* **2007**, *7*, 497–503.
- (18) Kiechner, C.; Liedl, T.; Kudara, S.; Pellegrino, T.; Javier, A. M.; Gaub, H. E.; Stolzle, S.; Fertig, N.; Parak, W. J. Cytotoxicity of colloidal CdSe and CdSe/ZnS nanoparticles. *Nano Lett.* **2005**, *5*, 331–338.
- (19) Rico, C. M.; Majumdar, S.; Duarte-Gardea, M.; Peralta-Video, J. R.; Gardea-Torresdey, J. L. Interaction of nanoparticles with edible plants and their possible implications in the food chain. *J. Agric. Food Chem.* **2011**, *59*, 3485–3498.
- (20) Albus, C.; Theissen, P.; Hellmich, M.; Griebenow, R.; Wilhelm, B.; Aslim, D.; Schicha, H.; Kohle, K. Long-term effects of a multimodal behavioral intervention on myocardial perfusion - a randomized controlled trial. *Int. J. Behav. Med.* **2009**, *16*, 219–226.
- (21) Merchant, S. S.; Prochnik, S. E.; Vallon, O.; Harris, E. H.; Karpowicz, S. J.; Witman, G. B.; Terry, A.; Salamov, A.; Fritz-Laylin, L. K.; Maréchal-Drouard, L.; Marshall, W. F.; Qu, L.-H.; Nelson, D. R.; Sanderfoot, A. A.; Spalding, M. H.; Kapitonov, V. V.; Ren, Q.; Ferris, P.; Lindquist, E.; Shapiro, H.; Lucas, S. M.; Grimwood, J.; Schmutz, J.; Team, C. A.; Team, J. A.; Grigoriev, I. V.; Rokhsar, D. S.; Grossman, A. R. The *Chlamydomonas* genome reveals the evolution of key animal and plant functions. *Science* **2007**, *318*, 245–251.
- (22) Harris, E. R. *Culture and storage method in the Chlamydomonas sourcebook-a comprehensive guide to biology and laboratory use*; Academic Press: San Diego, 1989.
- (23) Kola, H.; Wilkinson, K. J. Cadmium uptake by a green alga can be predicted by equilibrium modelling. *Environ. Sci. Technol.* **2005**, *39*, 3040–3047.
- (24) Kola, H.; Laglera, L. M.; Parthasarathy, N.; Wilkinson, K. J. Cadmium adsorption by *Chlamydomonas reinhardtii* and its interaction with the cell wall proteins. *Environ. Chem.* **2004**, *1*, 172–179.
- (25) Allison, J. D.; Brown, D. S.; Novo-Grada, MINTEQA2/PRODEFA2, A geochemical assessment model for environmental systems, version 3.0. In Office of Research and Development, U.S. Environmental Protection Agency: Athens, 1999; Vol. 3rd ed.
- (26) Hassler, C. S.; Slaveykova, V. I.; Wilkinson, K. J. Discriminating between intra- and extracellular metals using chemical extractions. *Limnol. Oceanogr. Methods* **2004**, *2*, 237–247.
- (27) Galceran, J.; Companys, E.; Puy, J.; Cecília, J.; Garcés, J. L. AGNES: a new electroanalytical technique for measuring free metal ion concentration. *J. Electroanal. Chem.* **2004**, *566*, 95–109.
- (28) Wilkinson, K. J.; Balnois, E.; Leppard, G. G.; Buffle, J. Characteristic features of the major components of freshwater colloidal organic matter revealed by transmission electron and atomic force microscopy. *Colloids Surf., A* **1999**, *155*, 287–310.
- (29) Balnois, E.; Papastavrou, G.; Wilkinson, K. J. Force microscopy and force measurements of environmental colloids. In *Environmental colloids: behaviour, structure and characterisation*; Wilkinson, K. J., Lead, J., Eds.; John Wiley & Sons, Ltd.: 2007; Vol. 10, pp 405–467.
- (30) Ondov, B. D.; Varadarajan, A.; Passalacqua, K. D.; Bergman, N. H. Efficient mapping of Applied Biosystems SOLiD sequence data to a reference genome for functional genomic applications. *Bioinformatics* **2008**, *24* (23), 2776–2777.
- (31) Li, H.; Ruan, J.; Durbin, R. Mapping short DNA sequencing reads and calling variants using mapping quality scores. *Genome Res.* **2008**, *18*, 1851–1858.
- (32) Atique, B.; Erb, M.; Gharabaghi, A.; Grodd, W.; Anders, S. Task-specific activity and connectivity within the mentalizing network during emotion and intention mentalizing. *Neuroimage* **2011**, *55*, 1899–1911.
- (33) Young, M. D.; Wakefield, M. J.; Smyth, G. K.; Oshlack, A. Gene ontology analysis for RNA-seq: accounting for selection bias. *Genome Biol.* **2010**, *11*, R14–R26.
- (34) Domingos, R. F.; Baalousha, M. A.; Ju-Nam, Y.; Reid, M. M.; Tufenkji, N.; Lead, J. R.; Leppard, G. G.; Wilkinson, K. J. Characterizing manufactured nanoparticles in the environment: multimethod determination of particle sizes. *Environ. Sci. Technol.* **2009**, *43*, 7277–7284.
- (35) Borm, P.; Klaessig, F. C.; Landry, T. D.; Moudgil, B.; Pauluhn, J.; Thomas, K.; Trottier, R.; Wood, S. Research strategies for safety evaluation of nanomaterials Part V: role of dissolution in biological fate and effects of nanoscale particles. *Toxicol. Sci.* **2006**, *90* (1), 23–32.
- (36) Slaveykova, V. I.; Wilkinson, K. J. Predicting the bioavailability of metals and metal complexes: critical review of the biotic ligand model. *Environ. Chem.* **2005**, *2*, 9–24.
- (37) Kariuki, S.; Dewald, H. D. Evaluation of diffusion coefficients of metallic ions in aqueous solutions. *Electroanalysis* **1996**, *8*, 307–313.
- (38) Wilkinson, K. J.; Buffle, J. Critical evaluation of physicochemical parameters and processes for modeling the biological uptake of trace metals in environmental (aquatic) systems. In *Physicochemical kinetics and transport at chemical - biological interfaces*; Leeuwen, H. P. v., Koester, W., Eds.; Wiley: Chichester, 2004; pp 445–533.
- (39) Li, J. M.; Timko, M. P. The pc-1 phenotype of *Chlamydomonas reinhardtii* results from a deletion mutation in the nuclear gene for NADPH:protochlorophyllide oxidoreductase. *Plant Mol. Biol.* **1996**, *30*, 15–37.
- (40) Li, K. G.; Chen, J. T.; Bai, S. S.; Wen, X.; Song, S. Y.; Yu, Q.; Li, J.; Wang, Y. Q. Intracellular oxidative stress and cadmium ions release induce cytotoxicity of unmodified cadmium sulfide quantum dots. *Toxicol. in Vitro* **2009**, *23*, 1007–1013.
- (41) Gagné, F.; Maysinger, D.; André, C.; Blaise, C. Cytotoxicity of aged cadmium-telluride quantum dots to rainbow trout hepatocytes. *Nanotoxicology* **2008**, *2*, 113–120.